

TUNABLE ULTRAVIOLET SOURCE FOR RESONANT PHOTOEMISSION SPECTROSCOPY*

B.A. ORLOWSKI, B.J. KOWALSKI, E. GUZIEWICZ
AND K. SZAMOTA-SADOWSKA

Institute of Physics, Polish Academy of Sciences
Al. Lotników 32/46, 02-668 Warszawa, Poland

(Received March 8, 1999)

The paper presents original experimental results which were chosen to present an application of the synchrotron radiation for study of engineering of the valence band electronic structure of the semimagnetic semiconductors. The results of the resonant photoemission study (Fano type resonance) of transition metal atoms ($3p-3d$ electrons transition) and rare earth atoms ($4d-4f$ electrons transition) incorporated into the volume of the II-VI and IV-VI compounds or deposited on clean surface of the CdTe crystal will be presented.

PACS numbers: 79.60.-i, 71.20.Nr, 73.20.At

1. Introduction

Synchrotron storage ring is a source of continuous electromagnetic radiation in a very wide range of radiation energy, starting from infrared, by visible, vacuum ultraviolet, soft X-ray up to hard X-ray [1,2]. The appearance of the tuneable source of radiation, provided by synchrotron, opens new opportunities for advanced studies in materials science. It refers to the studies of the crystalline structure as well as to the studies of electronic structure of the materials. Application of the continuous, tuneable light source gives the possibility to study particular resonance effects appearing for single atoms incorporated to the clusters, liquids, volume of the solids and its surface.

As an adequate example of the one group of the mentioned methods of the crystalline structure investigation the extended X-ray absorption fine structure (EXAFS) method can be used. In the EXAFS method, the absorption spectrum of a given constituent atom of the material is measured at

* Presented at the Cracow Epiphany Conference on Electron-Positron Colliders, Cracow, Poland, January 5-10, 1999.

the chosen X-ray absorption edge (usually K or L). Detailed analysis of the oscillatory part of the absorption coefficient, extracted from the high energy tail (more than 100 eV above the absorption edge) of the acquired absorption spectrum, ensures the fundamental parameters describing the local environment of the absorbing atom in a lattice, *i.e.* the nearest-neighbours (also second nearest neighbours or higher order) distances and the coordination number [3–6]. Therefore, EXAFS became especially useful in the studies of local atomic order in ternary and multinary alloy systems since it led to the verification of the bond length vs alloy composition dependence, which usually do not obey the simple Vegard law [4–6] and references therein).

As an example of electronic structure study is an application of the tuneable ultraviolet light source in the range of energy from 10 eV to the 200 eV in the new technique — Resonant Photoemission Spectroscopy (RPES) [7–14]. In this technique the radiation energy $h\nu$ is tuned to reach the resonant electron transition of the electron in the atom, to excite locally and selectively the electron in the atom chosen in the *e.g.* ternary crystal $\text{Cd}_{1-x}\text{Fe}_x\text{Te}$ or $\text{Pb}_{1-x}\text{Gd}_x\text{Te}$ (*e.g.* transition metal $3p$ – $3d$ electronic transition or rare earth atoms $4d$ – $4f$ electronic transition). For this particular resonant energy appears the increase of the elements (peaks or structures) of the measured energy distribution curve of photoemitted electrons. The increase of this elements gives the possibility to ascribe observed peak or structure as corresponding to the particular atom electrons contribution to the electronic structure of the valence band and to determine the binding energy of this peak. The paper presents the application of the tuneable source of ultraviolet radiation for study of the valence band electronic structure of clean surface and volume of the semiconductor compounds and to investigate the change of the structure caused by the introduction of the transition metal or rare earth metal on the clean semiconductor surface and/or into the volume of the crystal. The resonant photoemission spectroscopy will be presented as a tool to determine the contribution of the electrons of the localised orbital $3d$ of the atoms of transition metal or localised orbital of $4f$ electrons of the rare earth metal atoms to the valence band electronic structure. The experimental results will be presented for the case when the impurity atoms will be introduced to the volume of the crystal during the crystal growth by the modified Bridgman method ($\text{Cd}_{1-x}\text{Fe}_x\text{Te}$, $\text{Pb}_{1-x}\text{Gd}_x\text{Te}$ or $\text{Pb}_{1-x}\text{Eu}_x\text{Te}$) and to the case when the impurity atoms will be deposited on the clean surface of the semiconductor compound (Yb on CdTe).

2. Photoemission Electron Spectroscopy

The Fig. 1 presents the conditions of the photoemission experiment [7,8]. The sample is illuminated by the radiation in the energy $h\nu$ range between 20 and 200 eV. The angle of illumination is frequently 45° to the surface normal. The illumination of the sample leads to the photoemission of the electrons from the surface of the sample. The electron energy analyser can measure the Energy Distribution Curve (EDC) of the emitted electrons as a whole angle integrated total amount of the emitted electrons energy distribution or it can measure the energy distribution curve as a function of particular take-off angle (Angle Resolved AREDC). In the first case the angle integrated electronic structure will be measured while in the second case the band structure — $E(\vec{k})$ dependence can be determined from the measured curves.

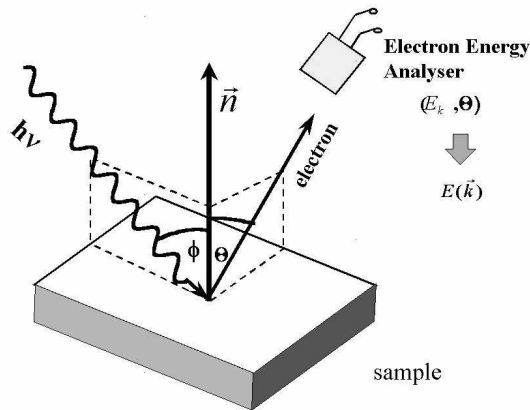


Fig. 1. The configuration of the photoemission experiment.

The ultraviolet radiation penetrates to the sample on the distance of the several hundred of Ångströms as the absorption coefficient for the radiation is in the range of 10^6 cm^{-1} (Fig. 2). The escape depth (the distance on which the number of escaping electrons decreases e times) of the electrons leaving the crystal strongly depends on the kinetic energy of the emitted electrons and it can range from several Ångströms up to several hundreds of Ångströms [7,8]. In a case when kinetic energy of escaping electron is about 90 eV, the escape depth reaches the minimum value of several Ångströms. This region of electron kinetic energy is commonly used to distinguish the surface effects contribution to the measured spectra. If becoming with kinetic energy more distant from 90 eV, the continuous and pronounced increase of the escape depth leads to the increase of the volume electrons contribution to the measured spectra.

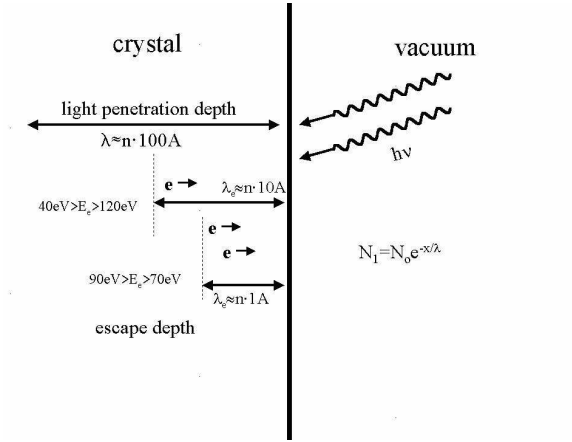


Fig. 2. The depth of the penetration of the ultraviolet radiation and the ranges of the value of the escape depth dependence on the kinetic energy of escaping electron.

Fig. 3 presents how the energy distribution curve is created by the electron energy analyser counting of the photoemitted electrons in the vacuum (at the right hand side of Fig. 3). The left hand side of Fig. 3 presents the density of states distribution in the crystal—below the vacuum level. The structure of the occupied states of the crystal is shifted of $h\nu$ energy to the vacuum.

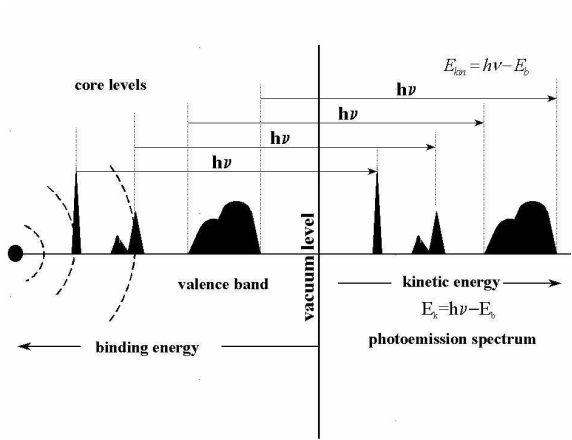


Fig. 3. The model how the energy distribution curve is created. The left hand side of the figure presents the density of occupied states distribution in the crystal — below the vacuum level. The structure of the occupied states of the crystal is shifted by $h\nu$ energy to the vacuum. The electron energy analyser counts the photoemitted electrons in the vacuum (right hand side of Fig. 3).

All the atoms adsorbed on the surface strongly scatter the escaping photoemitted electrons. To obtain the proper electronic structure of the crystal the crystal surface has to be clean. The best way to get a clean surface of the crystal is the cleavage of the crystal in the ultra high vacuum conditions and to perform the measurements in situ. The other method to obtain clean surface is the Ar ion bombardment of the crystal surface followed by heating. For some of the experiments the filing of the *e.g.* metallic sample is an efficient way of the sample surface cleaning.

3. Resonant Photoemission Spectroscopy

Tuneable radiation source gives the possibility to measure the ultraviolet absorption edge of the thin metallic films like *e.g.* the transition metal ($3p-3d$ electrons transition observed *e.g.* for Fe atoms for radiation energy around 57 eV [9]) or rare earth atoms ($4d-4f$ electrons transition observed for *e.g.* Gd atoms for energy of radiation around 150 eV [9]). The change of the Fe $3d^6$ or Gd $4f^7$ orbital occupation can be expressed in regular photoemission process (not resonant photoemission Fig. 4) as follows:

$$\text{Fe}\dots 3p^6 3d^6 + h\nu = \text{Fe}\dots 3p^6 3d^5 + e^- ,$$

$$\text{Gd}\dots 4d^{10} 4f^7 + h\nu = \text{Gd}\dots 4d^{10} 4f^6 + e^- .$$

In the case when $h\nu$ radiation energy approaches the value of the resonant energy, the absorption of the light leads to the additional absorption of the radiation and to the creation of excited state of the atom (*). The change of the electron orbital occupation is as follows (see Fig. 4):

$$\text{Fe}\dots 3p^6 3d^6 + h\nu = [\text{Fe}\dots 3p^5 3d^7]^* = \text{Fe}\dots 3p^6 3d^5 + e^- ,$$

$$\text{Gd}\dots 4d^{10} 4f^7 + h\nu = [\text{Gd}\dots 4d^9 4f^8]^* = \text{Gd}\dots 4d^{10} 4f^6 + e^- .$$

Due to the quantum interference of the states obtained in both ways of photoemission process for Fe or Gd atoms, the contribution of the $3d$ or $4f$ electrons respectively to the spectra manifests itself clearly by the Fano-type resonant enhancement. The Fano-type resonance [10] curve possesses the maximum for the resonant energy $h\nu r$ and the minimum value for antiresonant energy lower than $h\nu r$ on about several eV. Hence, the contribution of the Fe $3d^6$ or Gd $4f^7$ shell to the electronic structure of the crystal valence band can be characterised by the comparison of the photoemission spectra taken for the resonant and antiresonant radiation energy [11–14].

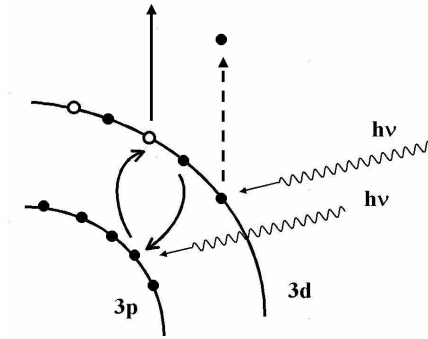


Fig. 4. Two possible ways of absorption of radiation at the resonant $h\nu$ energy region.

Fig. 5 presents the measured set of energy distribution curves corresponding to the electrons emitted from the valence band region (from valence band edge down to the 9 eV) of the ternary semimagnetic semiconductor crystal

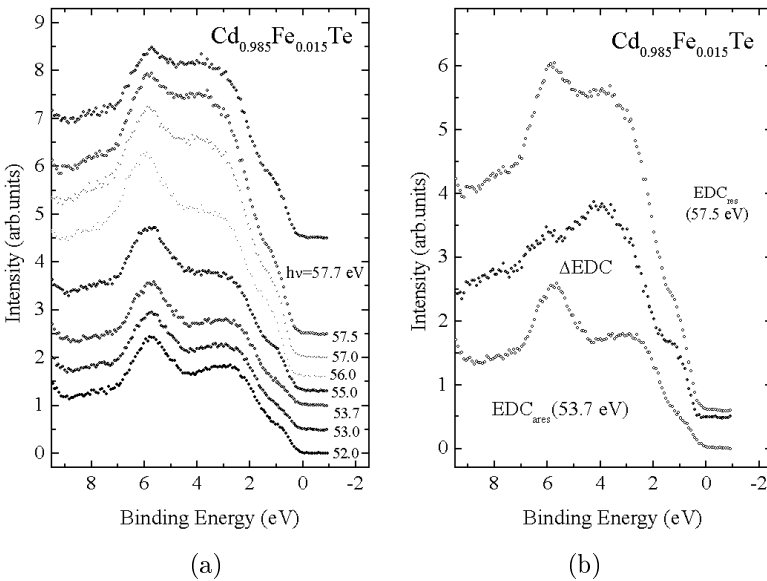


Fig. 5. Measured set of energy distribution curves corresponding to the electrons emitted from the valence band edge and down to the 9 eV of the ternary semimagnetic semiconductor crystal $\text{Cd}_{0.985}\text{Fe}_{0.015}\text{Te}$ for the different $h\nu$ energy indicated on the right hand side of the figure (a). The zero energy is located at the Fermi level. The curve ΔEDC was obtained by subtraction of the antiresonant curve (53.7 eV) from the resonance curve (57.5 eV).

$\text{Cd}_{0.985}\text{Fe}_{0.015}\text{Te}$. The zero of the binding energy is located at the Fermi level and the region of the energy down to the 7 eV corresponds to the width of the crystal valence band. In Fig. 5(a) each curve corresponds to the different $h\nu$ energy indicated on the right hand side of the figure. With an increase of the $h\nu$ value from 53.7 eV (antiresonant energy of the Fano type resonance) the contribution of 3d electrons to the curve increases and reaches the maximum for $h\nu$ equal 57.5 eV (resonant energy of the Fano type resonance) and then moderately decreases with increase of $h\nu$. In Fig. 5(b) the middle curve was obtained by subtraction of the antiresonant curve (53.7 eV) from the resonance curve (57.5 eV). This difference curve represents the contribution of the Fe 3d electrons to the electronic structure of the valence band of the ternary crystal $\text{Cd}_{0.985}\text{Fe}_{0.015}\text{Te}$.

Fig. 6 presents the measured set of energy distribution curves corresponding to the electrons emitted from the valence band region (from valence band edge down to the 15 eV) of the ternary semimagnetic semiconductor compounds crystals $\text{Pb}_{0.95}\text{Gd}_{0.05}\text{Te}$ (Fig. 6(a)) and $\text{Pb}_{0.95}\text{Gd}_{0.05}\text{Se}$ (Fig. 6(b)) [14]. The zero of the binding energy is located at the Fermi level and the whole energy region, up to 15 eV, corresponds to the width

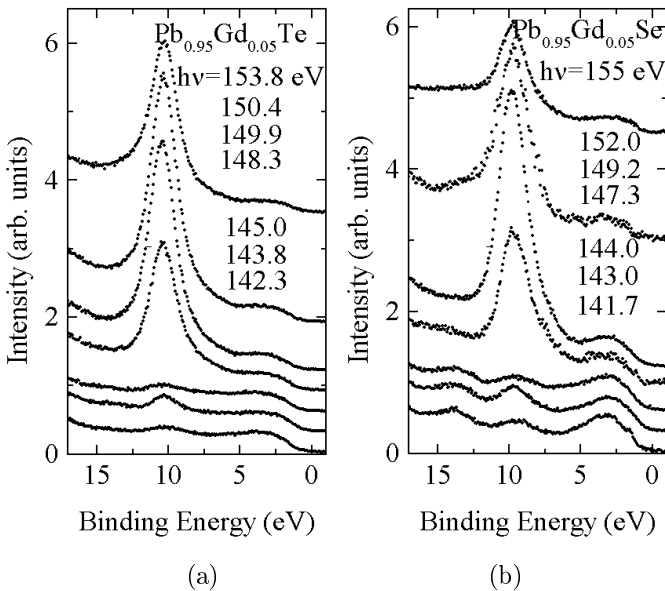


Fig. 6. Measured energy distribution curves corresponding to the electrons emitted from the valence band region (from valence band edge down to the 15 eV) of the ternary semimagnetic semiconductor compounds crystals $\text{Pb}_{0.95}\text{Gd}_{0.05}\text{Te}$ (a) and $\text{Pb}_{0.95}\text{Gd}_{0.05}\text{Se}$ (b).

of the crystal valence band. Changing the energy $h\nu$ from 142.3 eV up to 153.8 eV (Fig. 6(a)) we can recognise the resonant curve (biggest height of the peak corresponding to $4f^7$ electrons at the binding energy 10.2 eV) corresponding to the $h\nu = 150.4$ eV and antiresonant curve corresponding to the 145 eV. The difference between curves can be treated as a contribution of the electrons Gd $4f$ to the spectra.

Fig. 7 presents measured energy distribution curve corresponding to the electrons emitted from the valence band region of the ternary semimagnetic semiconductor compounds crystals $\text{Pb}_{0.95}\text{Eu}_{0.05}\text{Te}$ (Fig. 7(a)) and $\text{Pb}_{0.95}\text{Eu}_{0.05}\text{Se}$ (Fig. 7(b)). Changing the energy $h\nu$ from 128 eV up to 147 eV (Fig. 6(a)) we can recognise the resonant curve (peak corresponding to Eu $4f^7$ electrons located at the edge region of the valence band) corresponding to the $h\nu = 141.3$ eV and antiresonant curve corresponding to the $h\nu = 136$ eV.

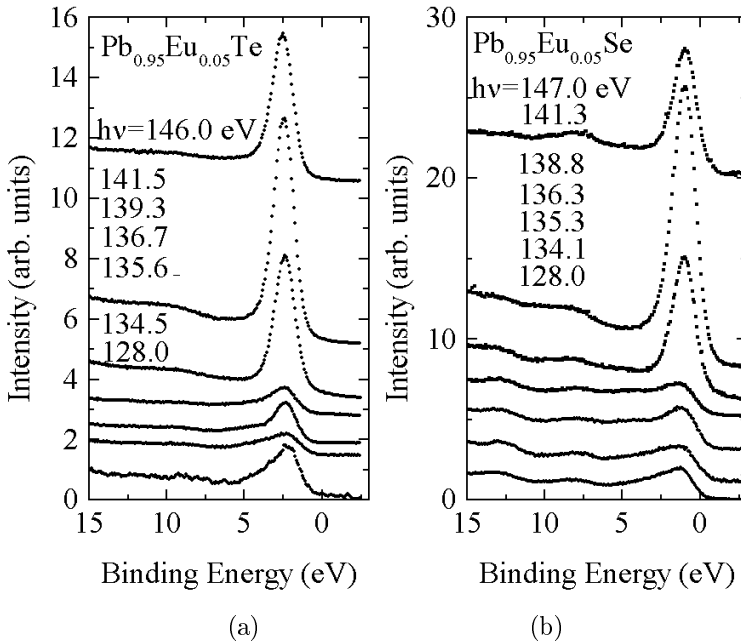


Fig. 7. Measured energy distribution curves corresponding to the electrons emitted from the valence band region of the ternary semimagnetic semiconductor compounds crystals $\text{Pb}_{0.95}\text{Eu}_{0.05}\text{Te}$ (a) and $\text{Pb}_{0.95}\text{Eu}_{0.05}\text{Se}$ (b).

The energy distribution curve corresponding to the electrons emitted from the valence band region of the CdTe crystal is presented on Fig. 8 curve A. The curve was taken for radiation energy $h\nu = 90$ eV for which the electron escape depth has the minimum. The zero of energy corresponds to

the valence band edge and two first peaks correspond to the valence band of CdTe crystal. The next peak corresponds to the Cd $4d$ electrons. After the deposition on its surface of about one monolayer of Yb atoms (curve B) the two split peaks of Yb $4f^{14}$ electrons dominates at the edge of the CdTe valence band region and the Yb layer dumps the height of the Cd $4d$ peak. After the heating of the sample the diffusion of the Yb atoms in the surface region takes place and the big part of Yb atoms deposited on the surface are now bonded to the Te atoms (curve C). On the curve C a new structure of the peaks appears (Yb $4f^{13}$) located below Yb $4f^{14}$ peak. This structure of the peaks corresponds to the split Yb $4f^{13}$ electrons. The change of the valence of Yb $^{2+}4f^{14}$ to the valence of Yb $^{3+}4f^{13}$ leads to the remarkable change of the contribution of the Yb $4f$ electrons to the valence band region spectra.

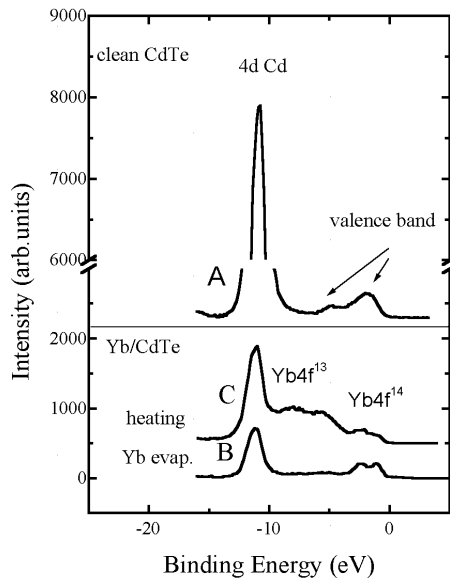


Fig. 8. Measured energy distribution curves ($h\nu = 90$ eV) corresponding to the electrons emitted from the valence band region of the CdTe crystal (A) and after deposition of Yb atoms on it (B) and then after heating (C).

4. Summary

The paper presents the examples of the application of the synchrotron radiation as a tuneable source of the ultraviolet radiation in the range from 20 to 200 eV, for study the electronic structure of the semimagnetic semiconductors ternary alloys by means of the resonant photoemission spectroscopy

using the Fano type resonance. The contribution of $3d$ electrons of Fe was determined for the Fe atoms introduced to CdTe crystal. The contribution of the $4f$ electrons of Gd or Eu atoms introduced to the PbTe and PbSe crystal valence band and Yb to the valence band of CdTe crystal was determined.

Authors acknowledge the support of KBN projects nr 2 P03B 089 10 and nr2 P03B 091 12.

REFERENCES

- [1] *Handbook of Synchrotron Radiation*, Vol. 1-4, Eds. D.E. Estman, Y. Farge, North-Holand, Amsterdam 1983-1991.
- [2] *Application of Synchrotron Radiation*, Eds. C.R.A. Catlow, G.N. Greaves, Blackie, Glasgow 1990.
- [3] B.K. Teo, *EXAFS: Principles and Data Analysis, Inorganic Chemistry Concepts*, Vol. 9, Springer, Berlin 1986.
- [4] R.J. Iwanowski, K. Lawniczak-Jablonska, Z. Golacki, A. Traverse, *Chem. Phys. Lett.* **283**, 313 (1998).
- [5] J.B. Boyce, J.C. Mikkelson, *J. Cryst. Growth* **98**, 37 (1989).
- [6] A. Balzarotti, N. Motta, A. Kisiel, M. Zinnal-Starnawska, M.T. Czyzyk, M. Podgorny, *Phys. Rev.* **B31**, 7526 (1985).
- [7] S. Hufner, *Photoelectron Spectroscopy, Springer Series in Solid-State Science* vol. 82, ed. M. Cardona, 1996.
- [8] *Photoemission in Solids I and II, Topics in Applied Physics*, vol.26 and 27, ed. L. Ley, M. Cardona, Springer-Verlag, Berlin, Heidelberg, New York 1979.
- [9] B. Sonntag, P. Zimmermann, *Rep. Prog. Phys.* **55**, 911 (1992).
- [10] U. Fano, *Phys. Rev.* **124**, 1866 (1961).
- [11] L.C. Davis, *Phys. Rev.* **B25**, 2912 (1982).
- [12] R.J. Lad, V.E. Henrich, *Phys. Rev.* **B39**, 13478 (1989).
- [13] E. Guziewicz, B.J. Kowalski, B.A. Orlowski, J. Ghijsen, Yu. Li-Ming, R.L. Johnson, *J. Electron Spectrosc. Relat. Phenom.* **88**, 321 (1998).
- [14] B.J. Kowalski, Z. Golacki, E. Guziewicz, B.A. Orlowski, J. Ghijsen, R.L. Johnson, *Inst. Phys. Conf. Ser.* **152G**, 885 (1998).